Photosensitization of nanoparticulate TiO2 using a Re(I)–polypyridyl complex: studies on interfacial electron transfer in the ultrafast time domain

ARTICLE *in* PHYSICAL CHEMISTRY CHEMICAL PHYSICS · MAY 2012

Impact Factor: 4.49 · DOI: 10.1039/c2cp24105f · Source: PubMed

PCCP

Cite this: *Phys. Chem. Chem. Phys.*, 2012, **14**, 8192–8198

www.rsc.org/pccp

PAPER

Photosensitization of nanoparticulate TiO_2 using a Re(I)-polypyridyl complex: studies on interfacial electron transfer in the ultrafast time domain†

Prasenjit Kar,[a] Tanmay Banerjee,[a] Sandeep Verma,[b] Anik Sen,[a] Amitava Das,*[a] Bishwajit Ganguly*[a] and Hirendra N. Ghosh*[b]

Received 23rd December 2011, Accepted 11th April 2012
DOI: 10.1039/c2cp24105f

We have synthesized a new photoactive rhenium(I)-complex having a pendant catechol functionality $[Re(CO)_3Cl(\mathbf{L})]$ (**1**) (**L** is 4-[2-(4′-methyl-2,2′-bipyridinyl-4-yl)vinyl]benzene-1,2-diol) for studying the dynamics of the interfacial electron transfer between nanoparticulate TiO_2 and the photoexcited states of this Re(I)-complex using femtosecond transient absorption spectroscopy. Our steady state absorption studies revealed that complex **1** can bind strongly to TiO_2 surfaces through the catechol functionality with the formation of a charge transfer (CT) complex, which has been confirmed by the appearance of a new red-shifted CT band. The longer wavelength absorption band for **1**, bound to TiO_2 through the proposed catecholate functionality, could also be explained based on the DFT calculations. Dynamics of the interfacial electron transfer between **1** and TiO_2 nanoparticles was investigated by studying kinetics at various wavelengths in the visible and near infrared regions. Electron injection into the conduction band of the nanoparticulate TiO_2 was confirmed by detection of the conduction band electron in TiO_2 ($[e^-]_{TiO_2^{CB}}$) and the cation radical of the adsorbed dye ($\mathbf{1}^{\bullet+}$) in real time as monitored by transient absorption spectroscopy. A single exponential and pulse-width limited (<100 fs) electron injection was observed. Back electron transfer dynamics was determined by monitoring the decay kinetics of $\mathbf{1}^{\bullet+}$ and $[e^-]_{TiO_2^{CB}}$.

1. Introduction

Polypyridyl complexes of d^6 transition metals (Ru^{II}, Os^{II}, Re^{I}) have been widely studied for many years because they display a rich photochemistry primarily due to their relatively long lived metal-to-ligand charge-transfer (MLCT) excited states, which further undergo redox reactions.[1–4] These complexes can be used as important photosensitizers[1–4] for energy- and electron-transfer reactions with possible applications either in light energy conversion, or as components of molecular electronic or photonic devices. Many of these processes associated with these complexes take place at the ultrafast time scale. An important example of such a process is photosensitization of semiconductor electrodes in solar cells, which starts with the electron injection from a MLCT excited state of a polypyridine complex to the conduction band of TiO_2.[5–7] In this regard, Ru(II)polypyridyl-complexes have been studied widely by innumerable research groups owing to the modest redox potential or energy for the $Ru_{d\pi} \rightarrow bpy_{\pi^*}$-based MLCT excited states, and wider absorption of the solar emission spectrum.[8–12] Analogous argument could also be true for influencing the dynamics of the sensitization of nanoparticulate TiO_2 by photoactive Re(I)-polypyridyl complexes. Among various Re(I)-polypyridyl complexes, those containing the $Re(CO)_3(bpy)X$ group (where the ligand, X, is typically a halide) have received attention because of their high stability, which has enabled them to be used as photocatalysts in bimolecular reactions.[13] Lian and co-workers[14] have verified the effect of pH on electron transfer reaction on a TiO_2 film surface sensitized by a Re-polypyridyl complex. They have also demonstrated[15] the effect of electronic coupling on the ET rate in TiO_2, sensitized by three adsorbates, $Re(\mathbf{L}_n)(CO)_3Cl$ [$\mathbf{L}_n$ is a modified dcbpy ligand with n = 0, 1, 3 CH_2 units between the bipyridine and carboxylate groups]. In this report, we have discussed the possibility of using a suitable derivative of $Re(CO)_3(bpy)X$ that could be anchored on TiO_2 surfaces for achieving a photoinduced interfacial electron transfer from the photoexcited state of the Re(I)-complex to the conduction band of the nanoparticulate TiO_2 ($CB[TiO_2]$). In a manner similar to that in N3 dye,[6] the optical absorption in the Re(I)-polypyridyl complex is dominated by a $Re_{d\pi} \rightarrow \mathbf{L}_{\pi^*}$-based MLCT band transition. We have used the previously reported ligand (**L**)[16] with pendant catechol functionality for synthesis of a new Re(I)-bipyridyl derivative for anchoring onto the TiO_2 surfaces. It is well documented in the literature

[a] *Central Salt and Marine Chemicals Research Institute (CSIR), Bhavnagar 364002, Gujarat, India. E-mail: amitava@csmcri.org, ganguly@csmcri.org*
[b] *Radiation and Photo Chemistry Division, Bhabha Atomic Research Center, Mumbai, India. E-mail: hnghosh@barc.gov.in*
† Electronic supplementary information (ESI) available. See DOI: 10.1039/c2cp24105f

that catecholate forms a strong charge transfer complex with TiO_2 and that actually facilitates the interfacial electron injection process from the Cat_π to the conduction band of the semiconductor surfaces.[17]

This proposition has also been substantiated by calculations using *ab initio* molecular orbital theory and density functional theory.[18] Experimental results indicate that catechol reacts with a TiO_2 surface to form a bidentate structure that is favored over dissociative or molecular adsorption on the (101) anatase surface. This was further corroborated on the basis of ZINDO/S calculations. Recent reports from two different groups, using *ab initio* DFT molecular dynamics simulations in combination with quantum dynamics calculations of electronic relaxation, suggest an efficient interfacial electron transfer in catechol–TiO_2-anatase nanostructures in the ultrafast time domain ($\tau_1 < 6$ fs).[17,18] In order to investigate the effect of the excited state potential on the interfacial electron transfer in catechol–TiO_2-nanostructured anatase surfaces, earlier we have compared the electron transfer dynamics using analogous Ru(II) and Os(II)-polypyridyl complexes.[7,19] In an effort to obtain more insight into this interfacial electron transfer dynamics, we have synthesized another new but analogous sensitizer molecule, $Re(CO)_3Cl$(**L**). We have carried out detailed transient absorption spectral studies for studying the dynamics of the interfacial electron transfer, which enabled us to observe the dynamics of the excited-state relaxation, formation of the oxidized complex, as well as to study the dynamics of the back electron transfer from the $e^-_{TiO_2}$ to the photogenerated oxidized metal centre.

2. Experimental section

(a) Materials

Titanium(IV) tetraisopropoxide {$Ti[OCH(CH_3)_2]_4$} (Aldrich, 97%), [$Re(CO)_5Cl$], 4,4′-dimethyl-2,2′-bipyridyl, 3,4-dimethoxy benzaldehyde, *n*-butyl lithium, disopropyl amine were procured from Sigma-Aldrich and used as received. Solvents like THF and isopropyl alcohol were dried and distilled prior to use. Nanopure water (Barnsted System, USA) was used for making aqueous solutions. All other reagents were of AR grade and procured from S.D. Fine Chemicals (India). HPLC grade acetonitrile (E. Merck, Bombay, India) was used for all spectrophotometric titrations. Solvents were degassed thoroughly with IOLAR grade dinitrogen gas before use in the preparation of standard solutions.

(b) Nanoparticle preparation

Nanometer-size TiO_2 was prepared by controlled hydrolysis of titanium(IV) tetraisopropoxide.[20] A solution of 5 mL of $Ti[OCH(CH_3)_2]_4$ dissolved in 95 mL of isopropyl alcohol (Aldrich) was added dropwise (1 mL min^{-1}) to 900 mL of nanopure water (2 °C) at pH 1.5 (adjusted with HNO_3). The solution was continuously stirred for 10–12 hours until a transparent colloidal solution was formed. This was concentrated at 35–40 °C with a rotary evaporator and then dried with nitrogen stream to yield a white powder. In the present work all colloidal samples were prepared after dispersing the dry TiO_2 nanoparticles in water (15 g L^{-1}).

(c) Femtosecond visible spectrometer

The femtosecond tunable visible spectrometer has been developed based on a multi-pass amplified femtosecond Ti:sapphire laser system from Avesta, Russia (1 kHz repetition rate at 800 nm, 50 fs, 800 μJ per pulse) and described in our earlier publications.[21] The 800 nm output pulse from the multi-pass amplifier is split into two parts to generate pump and probe pulses. In the present investigation we have used both 800 nm (fundamental) and it's frequency doubled 400 nm as excitation sources. To generate pump pulses at 400 nm one part of 800 nm with 200 μJ per pulse is frequency doubled in BBO crystals. To generate visible probe pulses, about 3 μJ of the 800 nm beam is focused onto a 1.5 mm thick sapphire window. The intensity of the 800 nm beam is adjusted by iris size and ND filters to obtain a stable white light continuum in the 400 nm to over 1000 nm region. The probe pulses are split into the signal and reference beams and are detected by two matched photodiodes with variable gain. We have kept the spot sizes of the pump beam and probe beam at the crossing point around 500 and 300 micron respectively. The excitation energy density (at both 800 nm and 400 nm) was adjusted to ~2500 μJ cm^{-2}. The noise level of the white light is about ~0.5% with occasional spikes due to oscillator fluctuation. We have noticed that most laser noise is low-frequency noise and can be eliminated by comparing the adjacent probe laser pulses (pump blocked *vs.* unblocked using a mechanical chopper). The typical noise in the measured absorbance change is about <0.3%. The instrument response function (IRF) for 400 nm excitation was obtained by fitting the rise time of the bleach of a sodium salt of *meso*-tetrakis(4-sulfonatophenyl)porphyrin (TPPS) at 710 nm and found to be 120 fs.

(d) Synthesis of tricarbonyl[4-{2-(4′-methyl-{2,2′}bipyridinyl-4-yl)-vinyl}-benzene-1,2-diol]chlororhenium, $Re(CO)_3$(**L**)Cl (**1**)

[$Re(CO)_5Cl$] (100 mg, 0.274 mmol) and **L** (88 mg, 0.29 mmol) were dissolved in 25 mL of dry tetrahydrofuran and refluxed for 6 hours with continuous stirring in an inert atmosphere. The solvent was then reduced to 2 mL and 20 mL of diethyl ether was added to it which precipitated a yellow solid. This was filtered off using a grade 4 sintered glass crucible, washed with ether and then air dried. The solid so obtained was further purified by column chromatography using silica as the stationary phase and acetonitrile as the eluent. Yield: 100 mg (60%). ESI-MS (*m*/*z*): calculated for $C_{22}H_{16}ClN_2O_5Re$ 610.03, observed 574.98 $[M–Cl]^+$; ^1H NMR (200 MHz, d_6-DMSO): δ (ppm) 9.53 (1H, br, –O*H*); 9.21 (1H, br, –O*H*); 8.84 (1H, s, $H_{3'}$ (bpy)); 8.82 (1H, s, H_3 (bpy)); 8.80 (1H, d, J = 3.8 Hz, H_6 (bpy)); 8.71 (1H, m, $H_{6'}$ (bpy)); 7.79–7.72 (2H, m, H (ethenyl), $H_{5'}$ (bpy)); 7.58 (1H, dd, J = 5.4 Hz, 0.8 Hz, H_5 (bpy)); 7.13 (1H, s, H_2 (phenyl)); 7.12–7.01 (2H, m, H (ethenyl) and H_6 (phenyl)); 6.81 (1H, d, J = 8 Hz, H_5 (phenyl)); 2.58 (3H, s, bpy-CH_3). IR (KBr pellet, cm^{-1}): 3391, 3292 ($\nu_{O–H}$), 2021, 1905 ($\nu_{C=O}$); elemental analysis: calculated for $C_{22}H_{16}ClN_2O_5Re$: C, 43.31; H, 2.64; N, 4.59%; found: C, 43.29; H, 2.67; N, 4.61%; $E_{1/2}$ = 1.35 V (*vs.* NHE in water).[22]

(e) Computational method

All calculations were performed with density functional program DMol3 in Material Studio (version 4.1) of Accelrys Inc.[23]

using GGA/PW91/DND[24] level of theory. The GGA/PW91/DND solvent calculations were performed with COSMO[25] using the gas-phase optimized geometries. The dielectric constant of acetonitrile (37.5) was applied. The cluster of the TiO_2 (Ti_4O_{17}) anatase (101) surface was built on the basis of previous studies to study the interaction of a Re-complex with pendant catechol functionality ($Re(CO)_3$(**L**)Cl).[26] Hydrogen saturators were used on oxygens with dangling bonds so that the cluster was a closed shell with neutral charge.

3. Results and discussion

(a) Synthesis

The synthetic methodology adopted for the synthesis of complex **1** is outlined in Scheme 1. **L** was synthesized by following a reported procedure.[8] The complex was synthesized by reacting **L** with $[Re(CO)_5Cl]$ in THF under reflux. The reaction mixture was concentrated and the desired complex was precipitated in its crude form by addition of diethyl ether. This was filtered and was further purified by column chromatography. The identity and desired purity of the complex were confirmed by the ^{1}H NMR, ES-MS and other analytical methods (ESI†).

(b) Spectroscopic properties: UV-vis absorption and cyclic voltametric studies

Fig. 1 shows the optical absorption spectra of **1** in acetonitrile. Apart from the absorption band in the visible region, a strong band at 292 nm was observed, which was attributed to an **L** based $\pi \rightarrow \pi^*$ transition. A broad absorption band between 360–440 nm is assigned to $d_{Re(I)} \rightarrow L_{\pi^*}$-based metal to ligand charge transfer (MLCT) transition.[27] Cyclic voltammogram was recorded for complex **1** where a $Re^{I/II}$-based redox process was found to be reversible and the $E_{1/2}$ value for this couple was evaluated as 1.35 V (*vs.* NHE in water). It was important to evaluate the excited state potential of the sensitizer dye molecule to understand the thermodynamic feasibility of the electron injection process from the excited singlet/triplet state(s) to the conduction band of the semiconductor particle (TiO_2). E_{0-0} transition energy was evaluated as 2.46 eV from the onset optical absorption band. Thus the excited state potential of −1.1 V ($[E(S^+/S^*) = [E(S^+/S)] - E_{0-0}$) for **1** was found to lie above the conduction band edge of the TiO_2 and confirms the thermodynamically feasible electron injection into the conduction band of TiO_2.

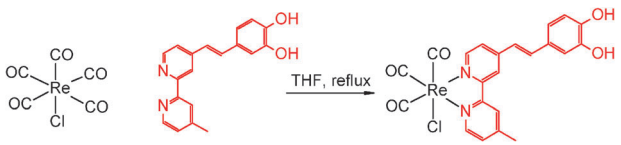

Scheme 1 Synthetic procedure followed for complex **1**.

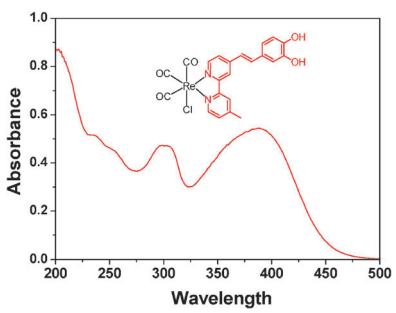

Fig. 1 Optical absorption spectra of complex **1** in acetonitrile. Inset: chemical structure of complex **1**.

(c) Dye binding with nanoparticles

In order to develop a better understanding of the interfacial electron transfer dynamics it is important to find the type of interaction between a sensitizer and TiO_2 nanoparticles in the ground state (Scheme 2). So it is essential to carry out optical absorption studies and compare spectra recorded in the absence and presence of TiO_2 nanoparticles. Fig. 2 shows the optical absorption spectra of **1** in aqueous solution and in dispersion of different concentrations of TiO_2 nanoparticles in aqueous solution. It is interesting to see that with increasing TiO_2 concentration a new 70 nm red-shifted band appears at 450 nm. A spectral band with λ_{max} at ~450 nm became more and more prominent with increasing amounts of added TiO_2. This new band could be attributed to the much lower HOMO–LUMO energy gap of the **1–TiO$_2$** complex owing to the very effective charge transfer type complex formation

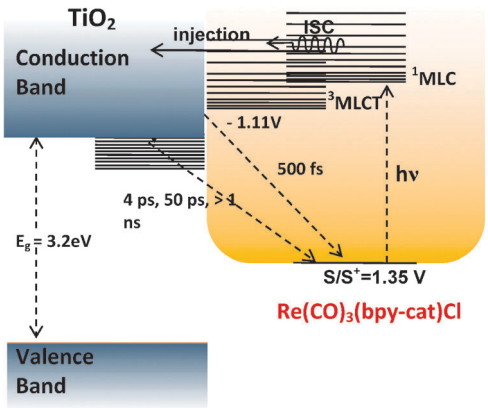

Scheme 2 Mechanistic scheme showing a three-level model, which consists of the ground state (S_o), the excited triplet state (^{3}MLCT) and the excited singlet state (^{1}MLCT) of **1**, bound to TiO_2^{NP}.

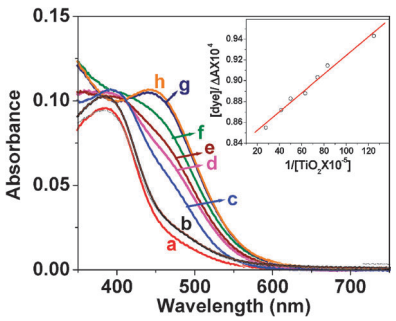

Fig. 2 Optical absorption spectra of complex **1** in the presence of various TiO_2 concentrations: (a) 0.001 g L^{-1}, (b) 0.003 g L^{-1}, (c) 0.01 g L^{-1}, (d) 0.015 g L^{-1}, (e) 0.02 g L^{-1}, (f) 0.025 g L^{-1}, (g) 0.075 g L^{-1}, (h) 0.1 g L^{-1}. Inset shows the Benesi–Hildebrand plot of the complex **1** sensitized TiO_2 system monitored at 462 nm.

between the TiO_2 and the pendant catecholate moiety. Formation of a strong charge transfer complex between the TiO_2 and catecholate functionality was also proposed earlier by us.[19] Earlier we have demonstrated that the interaction between TiO_2 nanoparticles and dye molecules like Ru-polypyridyl complex and Os-polypyridyl complex $[Os^{II}(bpy)_2(\mathbf{L})]$,[19] alizarin[21,28] and tri-phenyl methane (TPM) dyes[29] (pyrogallol red and bromo-pyrogallol red) is very strong. Interestingly, formation of a five membered ring and a charge transfer complex between catecholate functionality and TiO_2 is proposed by other researchers too. Thus, it can be conclusively emphasized that **1** interacts strongly with TiO_2 nanoparticles with the formation of a five-membered charge transfer complex. However, the shift observed for complex **1** was much more significant compared to those that we have observed earlier for CT complex formation for analogous Ru(II)- and Os(II)-polypyridyl complexes and TiO_2 nanoparticles. This might be due to strong CT interaction between the MLCT band of complex **1** and TiO_2 nanoparticles, where MLCT band transition is purely from Re metal to single **L** ligand. In our earlier studies with Ru(II)- and Os(II)-polypyridyl complexes,[7,19] the MLCT band used to consist of transition from $M^{2+}{}_{d\pi}$ to multiple bpy/$\mathbf{L}_{\pi^*}$ orbitals of ligands, as a result MLCT transition used to be delocalized between all the three ligands. In order to evaluate the binding constant for the binding of catecholate functionality to TiO_2, a systematic spectrophotometric titration was carried out by varying $[TiO_2{}^{NP}]$ (Fig. 2). The formation of a CT complex can be explained by the following equation:

$$TiO_2 + \mathbf{1} \rightarrow [TiO_2{}^{\delta-}\ldots\mathbf{1}^{\delta+}]_{Complex}$$

In the inset of Fig. 2, we have shown the Benesi–Hildebrand (B–H) plot, which was used to determine the molar extinction coefficient of the **1–TiO$_2$** complex, as well as the binding constant. Molar extinction coefficient and binding constants values were found to be 9.1×10^4 cm^{-1} M^{-1} and 7.8×10^3 M^{-1}, respectively.

(d) Computational studies

Recently, structural and electronic interactions between the sensitizer molecule and the TiO_2 nanocrystal have been reported using quantum chemical calculations.[18b,19c,30] These calculations provide insight for the interactions of the molecular orbitals of the sensitizer with the electronic bands of the substrate, which helps to rationalize experimental observations of ultrafast multiexponential photoinduced heterogeneous electron-transfer rates in these systems. Persson *et.al.* reported the charge transfer complex between catecholate and TiO_2 with quantum chemical calculations.[18b] We have examined the overall red shift of the observed MLCT band in binding of the Re-complex to TiO_2 computationally. Fig. 3 gives the Frontier molecular orbitals obtained for the free Re-complex (**1** and **1$_{Solvent}$**) and the one bound to the TiO_2 cluster (**1–TiO$_2$** and **1$_{Solvent}$–TiO$_2$**) in both gas and solvent phases. Employing density functional calculations, using the GGA/PW91/DND level, geometries were fully optimized and were taken for the orbital analyses. Orbital analyses showed that the orbital co-efficients of the metal centre and the co-ordinated CO and Cl ligands are largely located in HOMO-1 or HOMO-2 orbitals.[31] The Re-complex bound to the TiO_2 surface also showed similar trends in the gas and solvent phases.

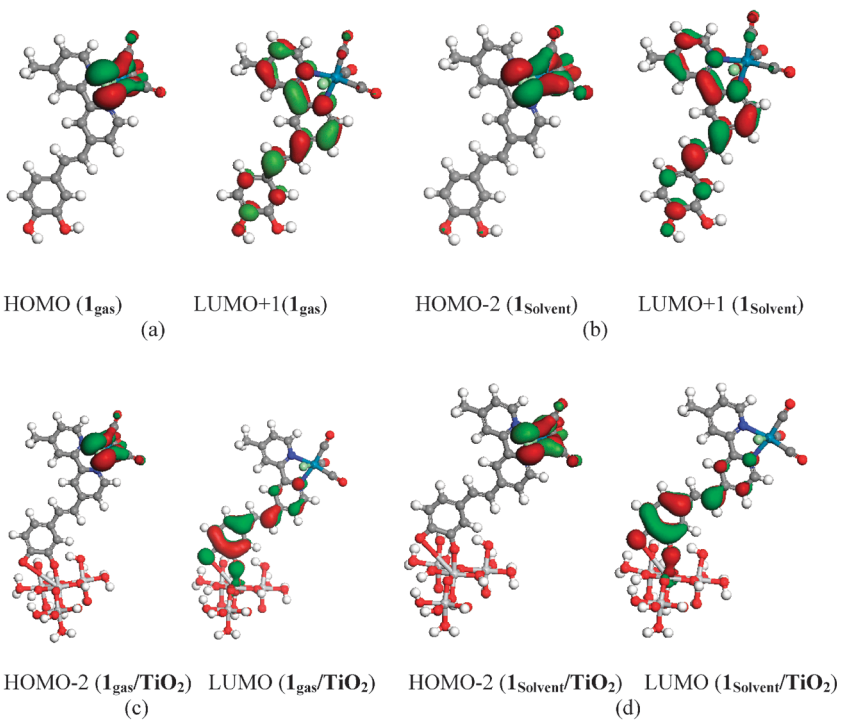

Fig. 3 GGA/PW91/DND calculated frontier molecular orbitals for $Re(CO)_3(\mathbf{L})Cl$ in (a) gas phase (**1$_{gas}$**) and (b) solvent phase (acetonitrile) (**1$_{Solvent}$**). (c) and (d) represent the frontier molecular orbitals of **1–TiO$_2$** (**1** bound to TiO_2) in gas (**1$_{gas}$–TiO$_2$**) and solvent phase (**1$_{Solvent}$–TiO$_2$**) respectively.

A larger coefficient was observed on the **L** for the LUMO orbital in the TiO_2 bound complex. The energy difference between the frontier orbitals for **1** in acetonitrile was predicted to be 2.56 eV, which is in agreement with the values observed (2.46) from the photoelectrochemical studies. The frontier orbital energy difference for the TiO_2 cluster bound complex (**1–TiO$_2$**) was found to be much smaller than the free one (1.009 eV). This result corroborates the shift of absorbance to the longer wavelength.

(e) Excited state dynamics of free complex 1

Photoinduced interfacial electron injection dynamics for the **1–TiO$_2$** system was studied using transient absorption spectral studies. To understand dynamics of the associated photo-induced processes involving photoexcited states of complex **1** and the CB[TiO_2^{NP}], it is essential to study the time resolved absorption spectra for the photoexcited states of complex **1** at different time delays in visible and near-IR regions. Fig. 4 shows the transient absorption spectra of **1** at different time delays in acetonitrile after excitation at 400 nm following our previous reports.[7,19] The excited state dynamics of the free dye could not be studied in water because of its very poor solubility. The excited state dynamics have also been studied in 10% acetonitrile and 90% water mixture and were found to be very similar to that in pure acetonitrile. In our earlier investigations[19b–d] we have observed that there is no effect on dynamics of ruthenium and osmium polypyridyl complexes by the variation in ACN and water solvent medium. The transients show a major broad absorption band in the wavelength region 500–900 nm with a hump at 550 nm. The transient absorption bands can be ascribed to the excited state absorption (ESA) of **1**. Due to higher spin–orbit coupling (calculated value for SO coupling of $Re(CO)_3(bpy)Cl$ is 503) in Re(I)-complexes (d^6 system) as compared to that of analogous Ru(II)-complexes, one would expect a more efficient and faster intersystem crossing (ISC) and relaxation within the excited state manifold. A more recent study revealed that the ISC process for an analogous Re(I)-complex happens within 85 fs.[32] For complex **1**, the primary optical transition associated with the excitation at 400 nm is a $Re_{d\pi} \rightarrow L_{\pi^*}$-based MLCT transition. This transition effectively oxidizes the Re(I) metal center to Re(II), which reduces the electron density on the metal center. So it is expected that excited absorption will be dominated by singlet ^{1}MLCT states of complex **1**. To understand the dynamics of the excited state following excitation at 400 nm, we have monitored kinetic decay traces at different wavelengths. The kinetic decay trace at 710 nm can be fitted multi-exponentially with different time constants with multi-exponential growth and decays. The growth signal can be fitted with 130 fs (78%) and 50 ps (22%) time components and the decay signal can be fitted with time 1.7 ps (13%) and >1 ns (87%). Assuming that ISC happens within $\lesssim$100 fs,[19,20] the response time of the excitation source, and the observed growth in absorbance in the present time resolved absorption studies at the 500–900 nm region can be attributed to the excited triplet state absorption (^{3}MLCT) (Fig. 4). The fast growth component is attributed to the formation of the hot ^{3}MLCT state after intersystem crossing conversion.[33] On the basis of ultrafast photophysics of metal polypyridine complexes, the slow component can be attributed to the vibrational cooling of the ^{3}MLCT state.[34] In our earlier investigations we have also observed a slow growth component in the transient signal of Ru(II)- and Os(II)-polypyridyl complexes,[9–12] which has been attributed to vibrational cooling. Interestingly in the present studies a second growth component was found to be much slower (50 ps) as compared to that of Ru(II)- and Os(II)-polypyridyl complexes.[7,19b,d] The longer vibrational cooling time in the Re(I)-complex in the present study might be due to the presence of smaller ligands (carbonyl and chloride) in addition to the single bpy-cat ligand. Further, reports on the photoexcited triplet state for the Re(I)-complex in the microsecond time domain have confirmed that the ^{3}MLCT state is long lived.[35]

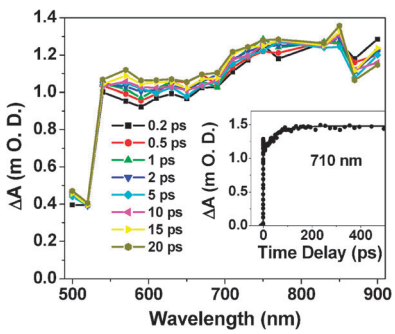

Fig. 4 Transient absorption spectra of **1** in acetonitrile at different delay times after excitation at 400 nm laser pulse. The transient spectrum shows a broad absorption band (490–1000 nm), which has been attributed to the ^{3}MLCT band (triplet–triplet absorption). Inset: kinetic trace of the excited triplet state (^{3}MLCT) of **1** at 610 nm.

(f) Transient absorption measurement of 1–TiO$_2$

We have carried out transient absorption experiments for complex **1** sensitized TiO_2 nanoparticles following excitation with a 400 nm excitation source. Time resolved absorption spectra recorded for **1–TiO$_2$** at different time delays on excitation at 400 nm are shown in Fig. 5. An appreciable bleaching in the TRA spectra at $\sim$470 nm was observed, while two broad absorption bands in the regions 500–730 nm and 730–1000 nm (with maxima at $\sim$940 nm) were observed. Time resolved studies revealed that the bleach at 470 nm and growth at 610 and 900 nm were pulse width limited and happen simultaneously and instantaneously following excitation with 400 nm laser pulse. As discussed earlier for analogous Re(I)-systems, the ISC process is known to happen within 85 fs.[32] Thus, it is reasonable to assume that hot excited triplet states get populated instantaneously (with the pulse width limit of the laser source of $\sim$100 fs) following excitation with the 400 laser source. The bleach at $\sim$470 nm and the transient absorption signal at 610 and 900 nm for **1–TiO$_2$** confirm electron transfer reaction between **1** and TiO_2 nanoparticles. A pulse-width limited single exponential growth and multi-exponential decay were observed at all wavelengths. In our earlier investigations,[7,19] we did confirm that for related Ru(II)/Os(II)-polypyridyl-complex/TiO_2 nanoparticle systems, the transient absorption spectra recorded are primarily due to the charge-separated species (cation radical ($1^{\bullet+}$) and injected

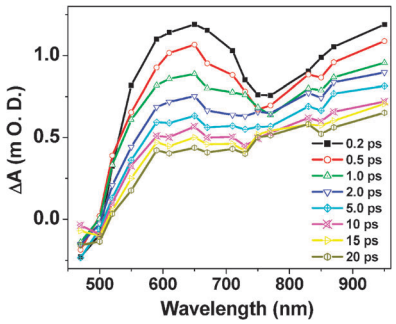

Fig. 5 Transient absorption spectra of **1–TiO$_2$** in water at different time delays after excitation at 400 nm. Typical concentration of **1** was ~200 μM, while that of TiO_2 nanoparticles was ~20 g L^{-1}.

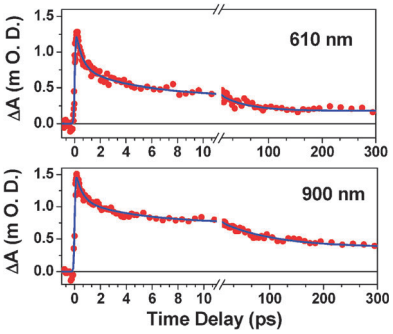

Fig. 6 Kinetic decay trace of the injected electron in the conduction band at 610 nm (upper panel) and at 900 nm (lower panel) of **1** sensitized TiO_2 nanoparticles.

electrons in TiO_2 ($e_{TiO_2}^-$)) and contribution due to excited states is very negligible. In these studies, it was indicated that electron injection took place predominantly from the non-thermalized singlet state (^{1}MLCT), and/or the non-thermalized triplet state (^{3}MLCT) or a combination of both, which is a unique observation in ET dynamics in Ru(II)-polypyridyl sensitized TiO_2 systems studied so far. Strong coupling in the dye–nanoparticle system facilitates ultrafast single exponential electron injection, which competes with the thermalization process of the excited states. If at all there is electron injection from the thermalized excited states, we could have seen the growth of the cation radical ($\mathbf{1}^{\bullet+}$) in the early time scale (<10 ps). However, we did not observe any such growth in transient absorption spectra. Lian and co-workers[36] also reported electron transfer reaction between the photoexcited state of the $Re(CO)_3Cl(dcbpy)$ complex and TiO_2 nanoparticles after monitoring a broad IR absorption of injected electrons after excitation at 400 nm. It was proposed that the electron injection from the photoexcited state of the Re(I)-complex can actually happen from the photoexcited thermally hot singlet and/or triplet states following a single exponential pathway with a concomitant growth of cation radicals within a time window of <100 fs. The rise time of the electron absorption signal was estimated to be <100 fs. In the present investigation also we have observed pulse-width limited (<100 fs) electron injection.

We have also monitored charge recombination dynamics which is a very important parameter in interfacial ET where injected electrons ($[e^-]_{TiO_2^{CB}}$) recombine with the radical cation center ($\mathbf{1}^{\bullet+}$). Recombination dynamics (BET) can be evaluated by monitoring the decay kinetics of either electrons in the conduction band at 900 nm, or the cation radical at 610 nm. Time constants for decay traces monitored at respective wavelengths are shown in Fig. 6. Kinetic decay traces for the cation radical ($\mathbf{1}^{\bullet+}$), monitored at 610 nm, could be best fitted multi-exponentially with time constants τ_1 = 0.5 ps (−42.8%), τ_2 = 4 ps (−25%), τ_3 = 50 (−19%) and τ_4 > 1 ns (−12%); while that for the decay trace at 710 nm could be fitted to a multi-exponential function with time constants τ_1 = 0.5 ps (−42.3%), τ_2 = 4 ps (−20.5%), τ_3 = 80 (−20.5%) and τ_4 > 1 ns (−16.7%). The kinetic decay traces at 900 nm were attributed to the charge recombination process involving $[e^-_{TiO_2^{CB}}]$ and $\mathbf{1}^{\bullet+}$. This could be fitted to a multiexponential function with time constants τ_1 = 0.5 ps (−30.8%), τ_2 = 4 ps (−19.7%), τ_3 = 100 (−26.5%) and τ_4 > 1 ns (−22.8%). It may be noted that the BET process observed for the present Re(I)-complex, **1**, is much faster when compared to that with $[Ru(bpy)_2(\mathbf{L}_1)]^{2+}$–$TiO_2$ and $[Os(bpy)_2(\mathbf{L}_1)]^{2+}$–$TiO_2$ systems.[7,19] This could be ascribed to the much stronger CT complex formation between **1** and TiO_2 as compared to that of the Ru(II)- and Os(II)-complex mentioned and this has been reflected in optical absorption studies where we have observed a new charge transfer band upon interaction with TiO_2 nanoparticles. In our earlier investigations[37] we have reported ultrafast BET dynamics in catechol sensitized TiO_2 nanoparticles where catechol forms a strong charge transfer complex with TiO_2 nanoparticles with formation of a new CT band in the ground state. Excitation of the CT band expedites ultrafast electron injection; while at the same time it facilitates the fast BET process. In all our studies[7,19] on interfacial electron transfer dynamics in TiO_2 nanoparticles and Ru(II)- and Os(II)-polypyridyl complexes with a pendant catechol moiety, we never observed a BET time constant component lower than 1.5 ps. However in the present investigation we have observed the fastest back ET time constant, which is as fast as 500 fs. HOMO–LUMO orbitals obtained from DFT calculations for **1** and the one bound to TiO_2 nanoparticles suggest that the orbital coefficients are largely concentrated on the catechol bound ring of **L** for the LUMO orbital and not spread out as found for the parent system. Our calculations clearly indicate that electron density mostly localized at the catecholate ligand bound to TiO_2. So majority of injected electrons in TiO_2 recombine with the parent cation radical ($\mathbf{1}^{\bullet+}$) before delocalization in TiO_2 nanoparticles. Our investigation is a unique example of localized electron transfer dynamics in a polypyridyl complex of transition metal ion sensitized TiO_2 nanoparticles which was never reported earlier in the literature.

4. Conclusion

We have synthesized a new Re(I)-complex (**1**) and studied the interfacial electron transfer dynamics between **1** and TiO_2 nanoparticles using femtosecond transient absorption spectroscopy. Steady state optical absorption spectroscopy suggests the strong binding of the sensitizer molecule to TiO_2^{NP}.

Upon excitation with 400 nm laser pulse, a bleach of the adsorbed dye, transient absorption of the dye cation ($\mathbf{1}^{\bullet+}$) and broad absorption band for the conduction band electron are observed. Electron injection is found to be single exponential and pulse width limited (<100 fs) indicating injection from the non-thermalized singlet state (^{1}MLCT), and/or the non-thermalized triplet state (^{3}MLCT) or a combination or both. Back ET dynamics was studied by monitoring the decay kinetics of the cation radical ($\mathbf{1}^{\bullet+}$), and injected electrons in the conduction band of TiO_2. Back ET reaction dynamics could be fitted multi-exponentially with time constants τ_1 = 0.5 ps (−30.8%), τ_2 = 4 ps (−19.7%), τ_3 = 100 (−26.5%) and τ_4 > 1 ns (−22.8%). In the present investigation we have observed that strong coupling between Re(I)-complex (**1**) and TiO_2 nanoparticles facilitates ultrafast back ET reaction, where injected electrons recombine with the parent cation radical ($\mathbf{1}^{\bullet+}$) before de-localization in TiO_2 nanoparticles. To the best our knowledge this is the first example of localized electron transfer dynamics in transition metal polypyridyl complex sensitized TiO_2 nanoparticles.

Acknowledgements

BRNS (DAE, India) and CSIR (India) have supported this work. PK acknowledges CSIR and AS acknowledges UGC for their Sr Research Fellowship. AD, BG and HNG thank Dr P. K. Ghosh (CSMCRI), Dr D. K. Palit (BARC), Dr S. K. Sarkar (BARC) and Dr T. Mukherjee (BARC) for their interest in this work.

References

1 R. J. D. Miller, G. L. McLendon, A. J. Nozik, W. Schmickler and F. Willig, *Surface Electron-Transfer Processes*, VCH, 1995.
2 A. J. Nozik and R. Memming, *J. Phys. Chem.*, 1996, **100**, 13061.
3 P. V. Kamat, *Prog. React. Kinet.*, 1994, **19**, 277.
4 A. Hagfeldt and M. Gratzel, *Chem. Rev.*, 1995, **95**, 49.
5 J. B. Asbury, E. Hao, Y. Wang, H. N. Ghosh and T. Lian, *J. Phys. Chem. B*, 2001, **105**, 4545.
6 B. O'Regan and M. Gratzel, *Nature*, 1991, **353**, 737.
7 G. Ramakrishna, D. A. Jose, D. K. Kumar, A. Das, D. K. Palit and H. N. Ghosh, *J. Phys. Chem. B*, 2005, **109**, 15445.
8 S. A. McFarland and N. S. Finney, *Chem. Commun.*, 2003, 388.
9 A. Juris, V. Balzani, F. Barigelletti, S. Campagna, P. Belser and A. von Zelewsky, *Coord. Chem. Rev.*, 1988, **84**, 85.
10 K. Kalyanasundaram, *Coord. Chem. Rev.*, 1982, **46**, 159.
11 K. Kalyanasundaram, *Photochemistry of Polypyridine and Porphyrin Complexes*, Academic Press, London, 1992, ch. 6.
12 A. Hagfeldt, G. Boschloo, L. Sun, L. Kloo and H. Pettersson, *Chem. Rev.*, 2010, **110**, 6595.
13 (*a*) J. Hawecker, J.-M. Lehn and R. Ziessel, *Helv. Chim. Acta*, 1986, **69**, 1990; (*b*) J. Hawecker, J.-M. Lehn and R. Ziessel, *J. Chem. Soc., Chem. Commun.*, 1983, 536; (*c*) F. P. A. Johnson, M. W. George, F. Hartl and J. J. Turner, *Organometallics*, 1996, **15**, 3374; (*d*) H. Takeda, K. Koike, H. Inoue and O. Ishitani, *J. Am. Chem. Soc.*, 2008, **130**, 2023.
14 C. She, N. A. Anderson, J. Guo, F. Liu, W.-H. Goh, D.-T. Chen, D. L Mohler, Z.-Q. Tian, J. T. Hupp and T. Lian, *J. Phys. Chem. B*, 2005, **109**, 19345.
15 J. B. Asbury, E. Hao, Y. Wang and T. Lian, *J. Phys. Chem. B*, 2000, **104**, 11957.
16 A. D. Shukla, B. Whittle, H. C. Bajaj, A. Das and M. D. Ward, *Inorg. Chim. Acta*, 1999, **285**, 89.
17 W. R. Duncan and O. V. Prezhdo, *Annu. Rev. Phys. Chem.*, 2007, **58**, 143–184.
18 (*a*) L. G. C. Rego and V. S. Batista, *J. Am. Chem. Soc.*, 2003, **125**, 7989; (*b*) P. Persson, R. Bergström and S. Lunell, *J. Phys. Chem. B*, 2000, **104**, 10348; (*c*) J. B. Benedict and P. Coppens, *J. Am. Chem. Soc.*, 2010, **132**, 2938; (*d*) Z. Guo, W. Z. Liang, Y. Zhao and G. H. Chen, *J. Phys. Chem. C*, 2008, **112**, 16655; (*e*) S. Köppen and W. Langel, *Phys. Chem. Chem. Phys.*, 2008, **10**, 1907; (*f*) W. R. Duncan and O. V. Prezhdo, *J. Phys. Chem. B*, 2005, **109**, 365; (*g*) R. Sánchez-de-Armas, J. Oviedo, A. S. Miguel and J. F. Sanz, *J. Phys. Chem. C*, 2011, **115**, 11293.
19 (*a*) S. Verma, P. Kar, A. Das, D. K. Palit and H. N. Ghosh, *J. Phys. Chem. C*, 2008, **112**, 2918; (*b*) P. Kar, S. Verma, A. Das and H. N. Ghosh, *J. Phys. Chem. C*, 2009, **113**, 7970; (*c*) P. Kar, S. Verma, A. Sen, A. Das, B. Ganguly and H. N. Ghosh, *Inorg. Chem.*, 2010, **49**, 4167; (*d*) S. Verma, P. Kar, A. Das, D. K. Palit and H. N. Ghosh, *Chem.–Eur. J.*, 2010, **16**, 611; (*e*) S. Verma, A. Ghosh, A. Das and H. N. Ghosh, *Chem.–Eur. J.*, 2011, **17**, 1561; (*f*) S. Verma, P. Kar, A. Das and H. N. Ghosh, *Chem.–Eur. J.*, 2011, **17**, 3458; (*g*) T. Banerjee, S. Rawalekar, A. Das and H. N. Ghosh, *Eur. J. Inorg. Chem.*, 2011, 4187.
20 (*a*) D. Bahnemann, A. Henglein, J. Lilie and L. Spanhel, *J. Phys. Chem.*, 1984, **88**, 709; (*b*) H. N. Ghosh, *J. Phys. Chem. B*, 1999, **103**, 10382.
21 G. Ramakrishna, A. K. Singh, D. K. Palit and H. N. Ghosh, *J. Phys. Chem. B*, 2004, **108**, 1701.
22 M. K. Nazeeruddin, S. M. Zakeeruddin and K. Kalyanasundaram, *J. Phys. Chem.*, 1993, **97**, 9607.
23 (*a*) B. Delley, *J. Chem. Phys.*, 1990, **92**, 508; (*b*) B. Delley, *J. Chem. Phys.*, 2000, **113**, 7756; (*c*) *Materials Studio DMOL3 Version 4.1*, Accelrys Inc., San Diego, CA.
24 (*a*) J. P. Perdew and Y. Wang, *Phys. Rev. B: Condens. Matter Mater. Phys.*, 1992, **45**, 13244; (*b*) Z. Wu, R. E. Cohen and D. J. Singh, *Phys. Rev. B: Condens. Matter Mater. Phys.*, 2004, **70**, 104112; (*c*) P. Ziesche, S. Kurth and J. P. Perdew, *Comput. Mater. Sci.*, 1998, **11**, 122; (*d*) W. Kohn, A. D. Becke and R. G. Parr, *J. Phys. Chem.*, 1996, **100**, 12974; (*e*) J. P. Perdew, K. Burke and M. Ernzerhof, *Phys. Rev. Lett.*, 1996, **77**, 3865.
25 (*a*) ed. A. Klamt, P. R. Schleyer and L. Allinger, Wiley, New York, 1998, vol. 2, p. 604; (*b*) A. Klamt, *J. Phys. Chem.*, 1995, **99**, 2224.
26 (*a*) P. C. Redfern, P. Zapol, L. A. Curtiss, T. Rajh and M. C. Thurnauer, *J. Phys. Chem. B*, 2003, **107**, 11419; (*b*) A. Vittadini, A. Selloni, F. P. Rotzinger and M. Grätzel, *Phys. Rev. Lett.*, 1998, **81**, 2954; (*c*) M. Lazerri, A. Vittadini and A. Selloni, *Phys. Rev. B: Condens. Matter Mater. Phys.*, 2001, **63**, 155409.
27 (*a*) L. A. Worl, R. Duesing, P. Chen, L. D. Ciana and T. J. Meyer, *J. Chem. Soc., Dalton Trans.*, 1991, 849; (*b*) S. V. Wallandael, R. J. Shaver, D. P. Rillema, B. J. Yoblinski, M. Stathis and T. F. Guarr, *Inorg. Chem.*, 1990, **29**, 1761; (*c*) J. V. Caspar, B. P. Sullivan and T. J. Meyer, *Inorg. Chem.*, 1984, **23**, 2104.
28 S. Kaniyankandy, S. Verma, J. A. Mondal, D. K. Palit and H. N. Ghosh, *J. Phys. Chem. B*, 2009, **113**, 3593–3599.
29 G. Ramakrishna, H. N. Ghosh, A. K. Singh, D. K. Palit and J. P. Mittal, *J. Phys. Chem. B*, 2001, **105**, 12786.
30 (*a*) P. Persson, M. J. Lundqvist, R. Ernstorfer, W. A. Goddard, III and F. Willig, *J. Chem. Theory Comput.*, 2006, **2**, 441; (*b*) L. Gundlach, R. Ernstorfer and F. Willig, *Phys. Rev. B: Condens. Matter Mater. Phys.*, 2006, **74**, 035324; (*c*) P. Persson and M. J. Lundqvist, *J. Phys. Chem. B*, 2005, **109**, 11918; (*d*) J. Li, M. Nilsing, I. Kondov, H. Wang, P. Persson, S. Lunell and M. Thoss, *J. Phys. Chem. C*, 2008, **112**, 12326.
31 L. Salassa, C. Garino, A. Albertino, G. Volpi, C. Nervi, R. Gobetto and K. I. Hardcastle, *Organometallics*, 2008, **27**, 1427.
32 (*a*) A. Cannizzo, A. M. Blanco-Rodriguez, A. E. Nahhas, J. Sebera, S. Zalis, A. Vlcek Jr and M. Chergui, *J. Am. Chem. Soc.*, 2008, **130**, 8967; (*b*) M. Bubsy, F. Hartl, P. Matousek, M. Towrie and A. Vlcek Jr, *Chem.–Eur. J.*, 2008, **14**, 6912.
33 J. K. McKusker, *Acc. Chem. Res.*, 2003, **36**, 876.
34 (*a*) N. H. Damrauer and J. K. McCusker, *J. Phys. Chem. A*, 1999, **103**, 8440; (*b*) G. B. Shaw, D. J. Styers-Barnett, E. Z. Gannon, J. C. Granger and J. M. Papanikolas, *J. Phys. Chem. A*, 2004, **108**, 4998; (*c*) W. Henry, *et al.*, *J. Phys. Chem. A*, 2008, **112**, 4537.
35 V. W.-W. Yam, C.-Y. Lau and L.-X. Wu, *J. Chem. Soc., Dalton Trans.*, 1998, 1461.
36 Y. Wang, J. B. Asbury and T. Lian, *J. Phys. Chem. A*, 2000, **104**, 4291.
37 M. C. Rath, D. K. Palit, T. Mukherjee and H. N. Ghosh, *J. Photochem. Photobiol., A*, 2009, **204**, 209.

